

Supplement of Biogeosciences, 14, 861–883, 2017  
<http://www.biogeosciences.net/14/861/2017/>  
doi:10.5194/bg-14-861-2017-supplement  
© Author(s) 2017. CC Attribution 3.0 License.



*Supplement of*

## **Attaining whole-ecosystem warming using air and deep-soil heating methods with an elevated CO<sub>2</sub> atmosphere**

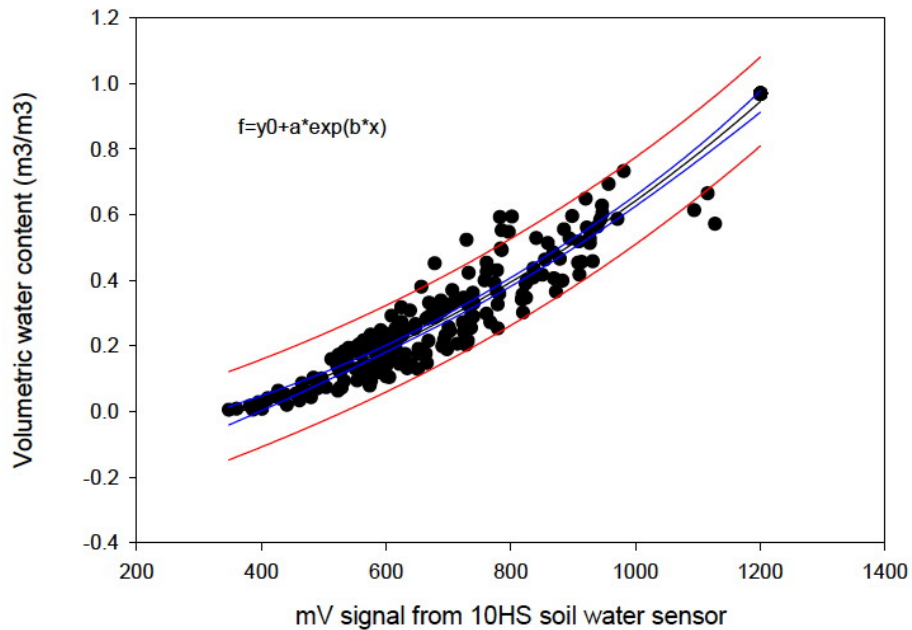
**Paul J. Hanson et al.**

*Correspondence to:* Paul J. Hanson ([hansonpj@ornl.gov](mailto:hansonpj@ornl.gov))

The copyright of individual parts of the supplement might differ from the CC-BY 3.0 licence.

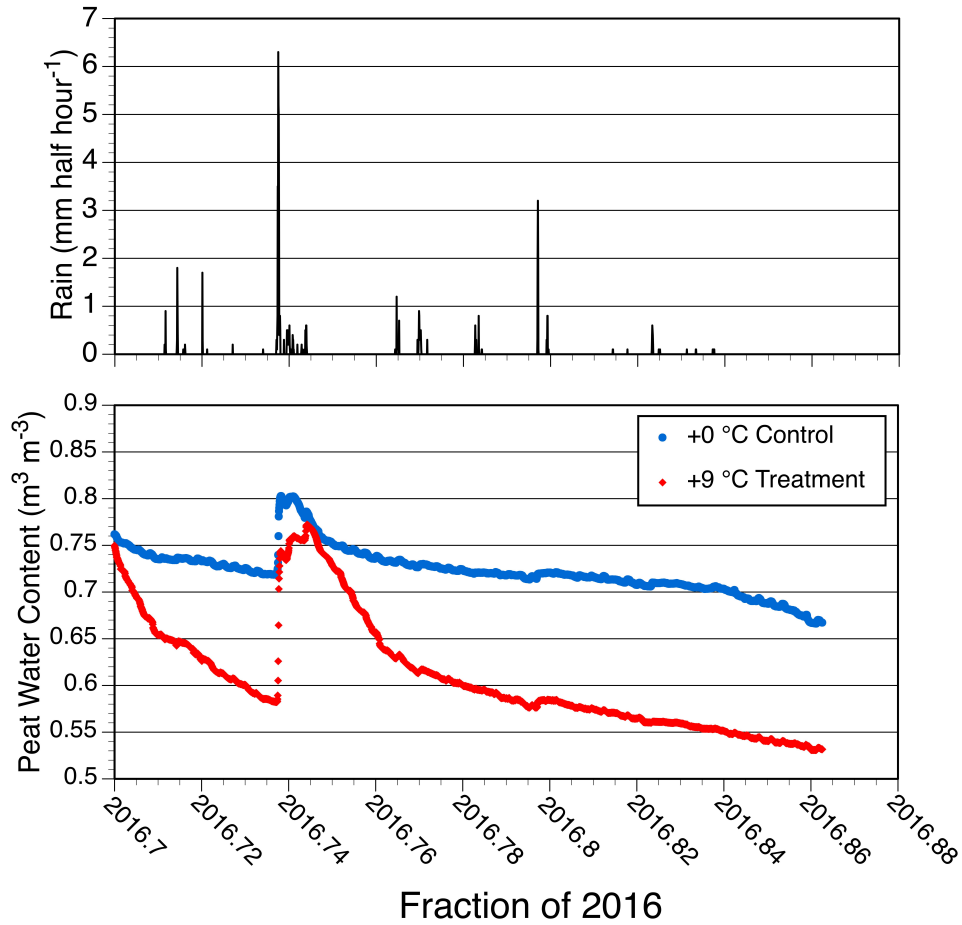
1 **Surface Peat Moisture Measurements (Jeff Warren)**

2 Intact *Sphagnum* peat monoliths were extracted from the S1-Bog into plastic containers (~7 L)  
3 and 10 replicates were taken to the Oak Ridge National Laboratory (ORNL) for calibration, and  
4 four replicates were sent to Decagon for factory calibration. One or two 10HS sensors were  
5 installed into each monolith, then water was added to the container to fully saturate the peat  
6 monolith and containers were placed into a plant growth chamber. Gravimetric water content  
7 was measured periodically as the monoliths dried down over several months and paired with the  
8 sensor mV output to create a custom calibration curve. During this period the *Sphagnum* surface  
9 (capitulum) water content was periodically assessed to derive a relationship between soil water  
10 content and surface water content – thereby providing data that is directly related to *Sphagnum*  
11 photosynthetic activity. The ORNL- and Decagon-based soil water calibration curves were  
12 similar, and using all 14 replicates resulted in a decent curve, where volumetric water content as  
13  $VMC = -0.731 + 0.508e^{(0.000995mV)}$  where mV is the voltage signal output from the sensors  
14 ( $R^2=0.92$ ; Supplemental Fig. S1).  
15



16 **Figure S1:** Calibration curve for the 10HS soil water sensor in peat.  
17  
18  
19

20 The dynamics of surface-peat drying are demonstrated in Figure S2 for a dry period in mid-  
21 summer 2016. Changes in peat soil water content are not evident for all rainfall events.  
22



23  
 24  
 25  
 26  
 27  
 28  
 29  
 30  
 31

**Figure S2:** Graph of half-hour rainfall at + 6 m (upper graph) and surface peat water content averaged over 0 to -10 cm (lower graph) during a mid-summer dry period during 2016. SE around the peat water content data are  $\pm 0.06$  to  $0.07 \text{ m}^3 \text{ m}^{-3}$ . Small precipitation events are intercepted by the canopy and peat *Sphagnum* surface and have limited effects on bulk water content observations.

32 **Spectral Characteristics of the SPRUCE Enclosure Glazing (D. M. Aubrecht)**

33 The spectral characteristics of the SPRUCE enclosure greenhouse panel glazing was evaluated  
34 from 250 nm to 20 microns using two radiometrically-calibrated directional hemispherical  
35 reflectance (DHR) spectrophotometers. One instrument measures UV/VNIR/SWIR (250 nm -  
36 2.5 micron) and the second measures mid- and long-wave infrared radiation (MWIR/LWIR; 2 -  
37 20 micron). All data include specular reflections.

38

39 The UV/VNIR/SWIR instrument is a Perkin-Elmer Lambda 750S spectrometer with a 100mm  
40 Spectralon integrating sphere and dual PMT and InGaAs detectors. The sample beam is incident  
41 at 8° from the sample surface normal. Data are collect at 1 nm resolution with 1 nm step size,  
42 and reflectance values are referenced to 99%R Spectralon. Data shown below are the mean of  
43 five independently sampled spectra.

44

45 The second instrument is a Thermo Scientific Nicolet iS10 FTIR spectrometer with a 3” Pike  
46 IntegratIR roughened gold integrating sphere and liquid nitrogen-cooled MCT detector. The  
47 sample beam strikes the sample surface at 12° from the surface normal. The sphere and internal  
48 beam path are purged with ultra pure dry nitrogen for 1 hour ahead of data collection in order to  
49 minimize absorption signals from CO<sub>2</sub> and H<sub>2</sub>O in the atmosphere. Individual spectra are the  
50 mean of 64 samples are referenced to roughened gold. Data are presented at 4 cm<sup>-1</sup> resolution  
51 and plots below are the mean of 10 independently sampled individual spectra.

52

53 Figure S3, below plots the greenhouse panel reflectance in comparison to the incoming solar  
54 spectrum (NREL “Global Tilt” data which accounts for all the solar energy that will interact with  
55 the SPRUCE enclosures), and the ideal blackbody radiation spectrum emitted by objects at 30 °C  
56 and 0 °C. There are two panel curves in the 2 – 2.5 micron region, where the two  
57 spectrophotometers overlap. Though the instruments give slightly different values, the overall  
58 magnitudes are in good agreement. Transmission data was also collected for the UV/VNIR, but  
59 is not shown. Transmission data for the MWIR was not collected, since at those wavelengths, the  
60 panels absorb all energy that they do not reflect.

61

62 We note the following characteristics of the greenhouse panels:

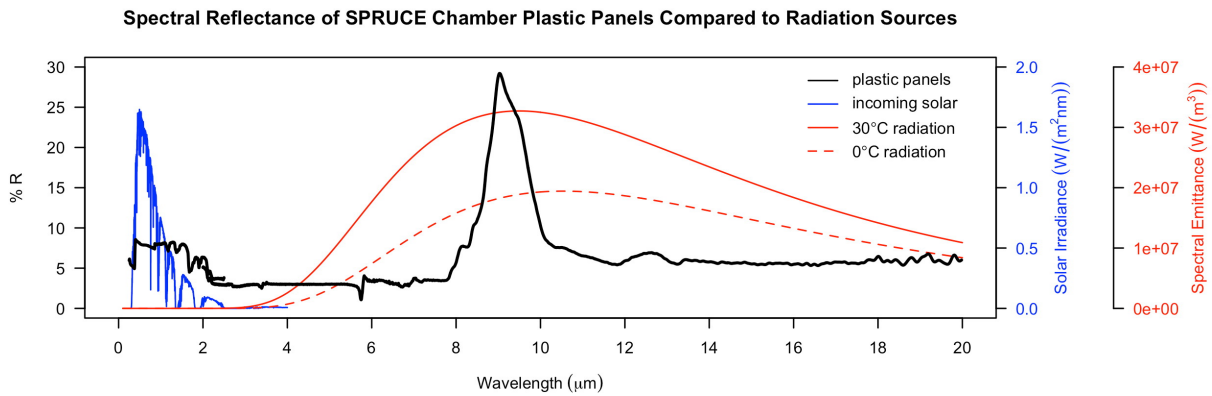
- 63 1) the panels absorb most of the UV and prevent it from entering the SPRUCE  
64 enclosures,
- 65 2) the panels transmit the majority of VNIR radiation and reflect only a small portion at  
66 these wavelengths,
- 67 3) the panels absorb >90% of the incoming MWIR/LWIR radiation (>3 microns), and  
68 4) the one part of the MWIR spectrum the panels reflect coincides with the peak of  
69 thermal radiation from objects that are 0-30°C (8-10 microns).

70

71 As the SPRUCE greenhouse panels transmit most of the VNIR wavelengths, PAR is reduced  
72 inside the enclosure, but only minimally. In the MWIR/LWIR, the story becomes more  
73 complicated. Since and the enclosure walls absorb most of the incoming radiation, the panels are  
74 likely a couple of degrees warmer than ambient air temperature when the sun is shining. In  
75 addition, the panels have a strong reflection feature at ~9 microns that reflects a fraction of the  
76 thermal energy emitted by the air, vegetation, and enclosure walls is back into the enclosure.

77 Thermal energy from the interior that is not reflected ends up being absorbed by the panels and  
78 reemitted back into the chamber.

79  
80 Therefore, the presence of the SPRUCE enclosure walls do not have a drastic effect on ambient  
81 PAR for the enclosed vegetation (20% reduction, as shown in Fig. 11), with the exception of  
82 shadows cast by the structure. However, the enclosure will minimize heat loss to the  
83 surroundings, and keep surface conditions within the enclosures warmer day and night than  
84 similar surfaces in the bog that are fully open to the sky. Since the frustum opening restricts  
85 radiation losses to the sky (in terms of solid angle), the interior of the enclosure cool slower than  
86 unchambered ambient plots, and the interior microenvironment of the enclosure behaves more  
87 like the understory of a closed forest canopy. Instead of seeing 180° of cold, clear sky, as the  
88 unchambered ambient plots do, the interior of SPRUCE enclosures experience a warmer  
89 apparent sky temperature with increased incoming longwave radiation, as shown in Fig. 12.  
90



91  
92 **Figure S3:** Spectral reflectance of SPRUCE enclosure plastic panels compared to radiation  
93 sources.

94  
95  
96

97 **Air warming PID details**  
98  
99 MAU\_Control = TA\_2M\_AVG\_5minAmb + (Temp\_target + Bias\_Air)  
100 AirTemp\_Diff = TA\_2M\_AVG\_5min - TA\_2M\_AVG\_5minAmb  
101 PID\_Diff\_Air = MAU\_Control - TA\_2M\_AVG\_5min  
102 I\_Air = I\_Air + P\_Air  
103 If I > MaxI\_Air Then I = MaxI\_Air  
104 If I < -MaxI\_Air Then I = -MaxI\_Air  
105 P\_Air\_Output = P\_Air \* PFact\_Air  
106 I\_Air\_Output = I\_Air \* IFact\_Air  
107 PID\_Scale = The range of temperature to scale the 4 to 20 mA control signal for the LP gas  
108 furnaces.  
109 Bias\_Air = offset  
110  
111 Code from the Campbell Logger  
112  
113 P\_Air = PID\_Diff\_Air  
114 I\_Air = I\_Air + P\_Air  
115 If I\_Air = NAN Then I\_Air = 0  
116 If I\_Air > MaxI\_Air Then I\_Air = MaxI\_Air  
117 If I\_Air < -MaxI\_Air Then I\_Air = -MaxI\_Air  
118 P\_Air\_Output = P\_Air \* PFact\_Air  
119 I\_Air\_Output = I\_Air \* IFact\_Air  
120 PID\_Air\_Output = ((P\_Air\_Output + I\_Air\_Output) \* PID\_Scale\_Air) - 3000  
121  
122 The 4 to 20 mA interface is scaled as -3000 = 4 mA and 5000 = 20 mA  
123 5000 + 3000 = 8000  
124 20 - 4 = 16  
125 16 / 8000 = .002  
126  
127 Example ((5000 + 3000) \* 0.002) + 4 = 20  
128  
129 PID\_Scale Example (1)  
130 If we want the range of control to be 0.6 degrees C Then 8000 / 0.6 = 13333.333  
131  
132 PID\_Scale Example (2)  
133 If we want the range of control to be 3.0 degrees C Then 8000 / 3 = 2666.6666  
134  
135 Table S1. Air Temperature PID Control Settings

Treatment	Plot #	P_Fact_Air	I_Fact_Air	PID_Scale_Air	MaxI_AIR	Bias_Air
+2.25	Plot_11	0.25	0.015	8000	20	0.02
+2.25	Plot_20	0.25	0.015	8000	20	0
+4.5	Plot_4	0.3	0.08	3555.5555	20	0
+4.5	Plot_13	0.3	0.1	3555.5555	20	0
+6.75	Plot_8	0.4	0.03	2666.6666	20	0

+6.75	Plot_16	0.4	0.04	2666.6666	20	0
+9	Plot_10	0.25	0.025	2666.6666	30	0
+9	Plot_17	0.3	0.025	5333.3333	30	0

136

137 Control settings for air temperature control as seen in Table S1. Air Temperature PID Control  
 138 Settings are very similar but not always the same for the same treatments. This may be explained  
 139 by slight differences in wind patterns across the S1 bog, differences in the efficiencies of the LP  
 140 gas furnaces, and vegetation differences inside the individual plots.

```

141 Soil warming PID details
142
143 PV = Process Variable (TS_200cm) A,B or C Probes
144 P = (TS_200cm_Amb_Avg + Temp Treatment) - PV
145 I = I + P
146 If I > MaxI Then I = MaxI
147 If I < -MaxI Then I = -MaxI
148 P_Output = P * Pfact
149 I_Output = I * Ifact
150 PID_Scale = The range of temperature to scale the 4 to 20 mA control signal for the SCR's
151 Bias_A(B,C) = offset
152
153 Code from Logger Program
154
155 RingA = TS_200cm_Amb_Avg + (Temp_target + Bias_A)
156 PID_Diff_A = RingA - A_200cm
157 P_A = PID_Diff_A
158     I_A = I_A + P_A
159     If I_A > MaxI Then I_A = MaxI
160     If I_A < -MaxI Then I_A = -MaxI
161     P_A_Output = P_A * PFact_A
162     I_A_Output = I_A * IFact_A
163     PID_A_Output = ((P_A_Output + I_A_Output) * PID_Scale_A) - 3000
164
165 The 4 to 20 mA interface is scaled as -3000 = 4 mA and 5000 = 20 mA
166 5000 + 3000 = 8000
167 20 - 4 = 16
168 16 / 8000 = .002
169
170 Example ((5000 + 3000) * 0.002) + 4 = 20
171
172 PID_Scale Example (1 )
173 If we want the range of control to be 0.6 degrees C Then 8000 / 0.6 = 13333.333
174
175 PID_Scale Example (2 )
176 If we want the range of control to be 3.0 degrees C Then 8000 / 3 = 2666.6666
177
178

```

179 Table S2. Soil temperature PID control settings

Treatment	Plot #	P_Fact_ A	I_Fact_ A	PID_Scale A	P_Fact_ B	I_Fact_ B	PID_Scale B	P_Fact_ C	I_Fact_ C	PID_Scale C	MaxI	Bias_ A	Bias_ B	Bias_ C
+2.25	PLOT_11	0.6	0.0015	4000	0.6	0.0015	4000	0.6	0.0015	4000	100	0	0	0.11
+2.25	PLOT_20	0.6	0.0015	4000	0.6	0.0015	4000	0.6	0.0015	4000	100	0	0	0
+4.5	PLOT_4	1.5	0.0011 3	3555.5555	1.6	0.0011 3	3555.5555	1.85	0.0011 3	3555.555	100	0	0.07	0.07
+4.5	PLOT_13	1.65	0.0011 3	3555.5555	1.6	0.0011 3	3555.5555	1.85	0.0011 3	3555.5555	100	0.15	0	0.1
+6.75	PLOT_8	2.1	0.0085	2666.6666	2.1	0.0015	2666.6666	2.2	0.0015	2666.6666	100	0.12	0.15	0.3
+6.75	PLOT_16	2.1	0.0035	2666.6666	0.0015	0.0085	2666.6666	0.0015	0.003	2666.6666	100	0.26	0.2	0.15
+9	PLOT_10	2.1	0.0015	2666.6666	2.1	0.0015	2666.6666	1.7	0.0015	2666.6666	100	0.0	0.43	0.2
+9	PLOT_17	2.1	0.0015	2666.667	2.1	0.0015	2666.667	1.7	0.0015	2666.667	100	0.0	0.13	0.34

180  
181

182 Table S3. Time required to reach DPH differentials by treatment plot.

Plot	Treatment (°C)	Date Soil Temp Monitoring Began	Date Treatment Began	Time Treatment Began (CST)	Days to Achieve Target °C Differentials for A and B Series within each plot
6	Control (+0)	2/25/14	NA	NA	0
19	Control (+0)	6/18/14	NA	NA	0
10	+9	5/19/14	6/17/14	14:00	81
17	+9	6/9/14	6/17/14	16:00	66
8	+6.75	5/20/14	6/25/14	9:30	94
16	+6.75	6/9/14	6/23/14	15:55	71
4	+4.5	2/25/14	7/2/14	13:00	58
13	+4.5	5/20/14	6/26/14	13:30	51
11	+2.25	5/20/14	7/1/14	13:00	22
20	+2.25	6/17/14	6/25/14	10:00	24

183  
184  
185

186

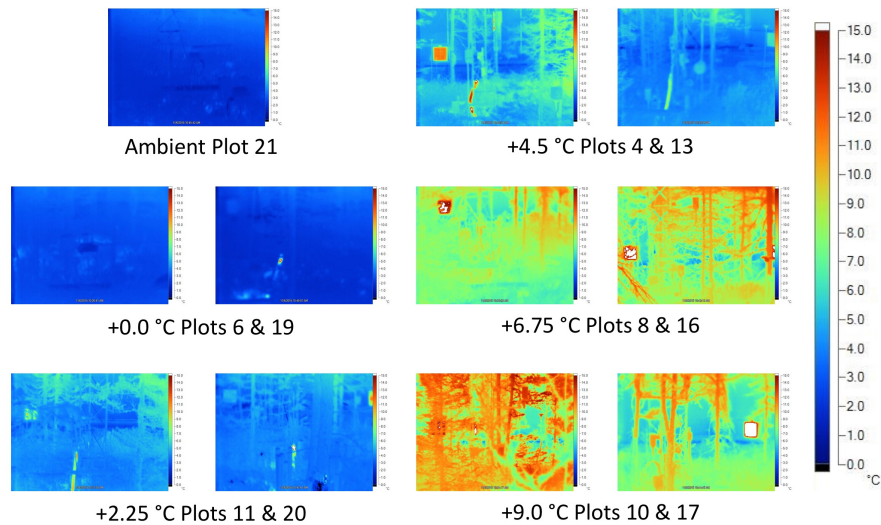


187  
188  
189  
190  
191  
192  
193

**Figure S4:** Left photograph is a completed SPRUCE warming enclosure, and the right photograph shows the subtending hydrologic corral that lies beneath each enclosure. The encircling and interlocked sheet piles extend through the peat to the ancient lake bed below, and effectively isolate the hydrology of the enclosure.

### Whole Ecosystem Warming In Pictures

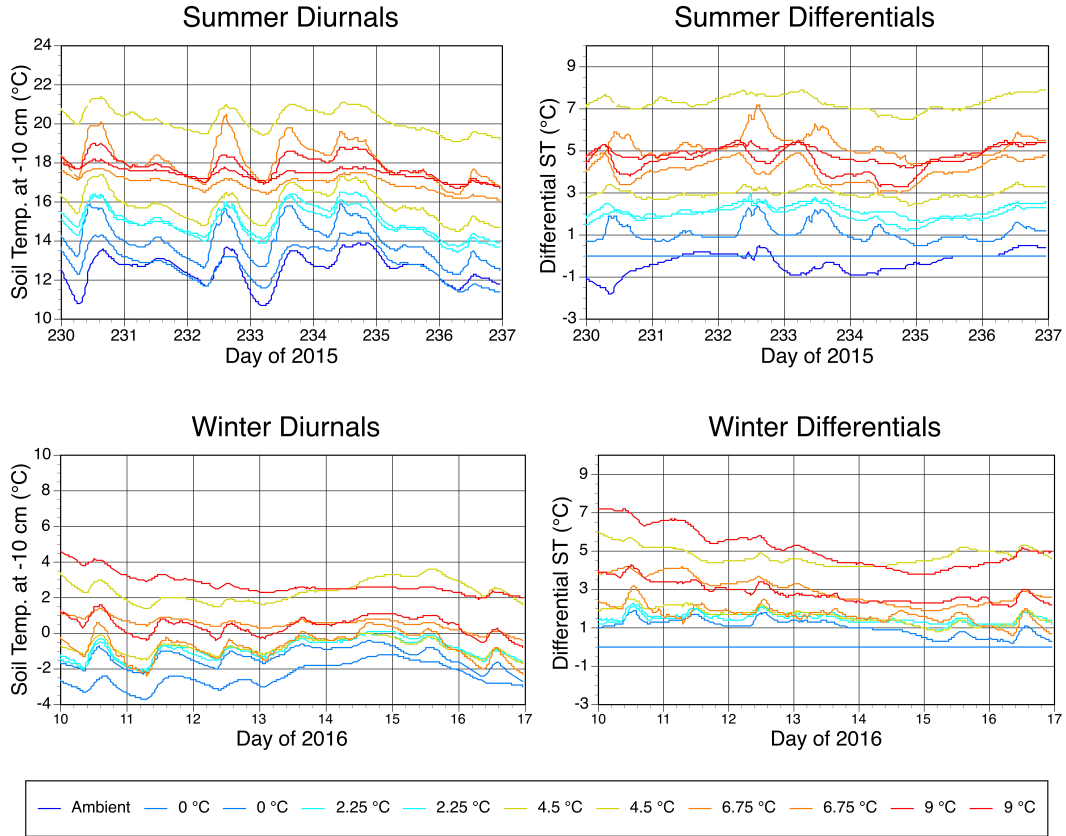
(6 November 2015; IR thermal Images)



194  
195  
196  
197  
198  
199  
200

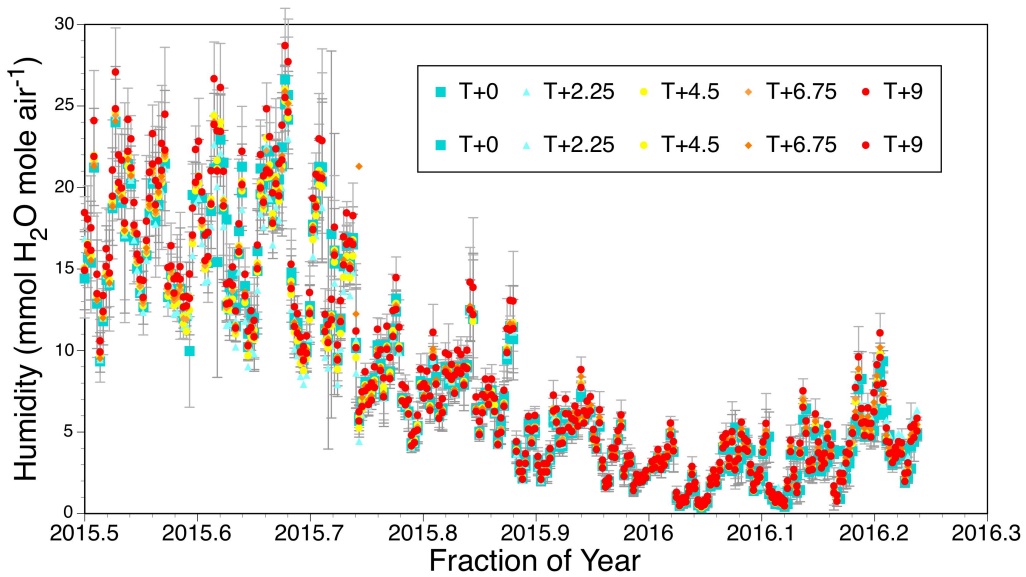
**Figure S5:** Color infrared images for the space within the designated treatment enclosures and an unchambered ambient plot recorded on November 6, 2015 just before sunrise within a 30-minute period. The thermal color scale in °C applies to all images. Non-biological metal or plastic surfaces in the images may not provide an accurate temperature due to their emissivity difference from biological surfaces.

201  
202



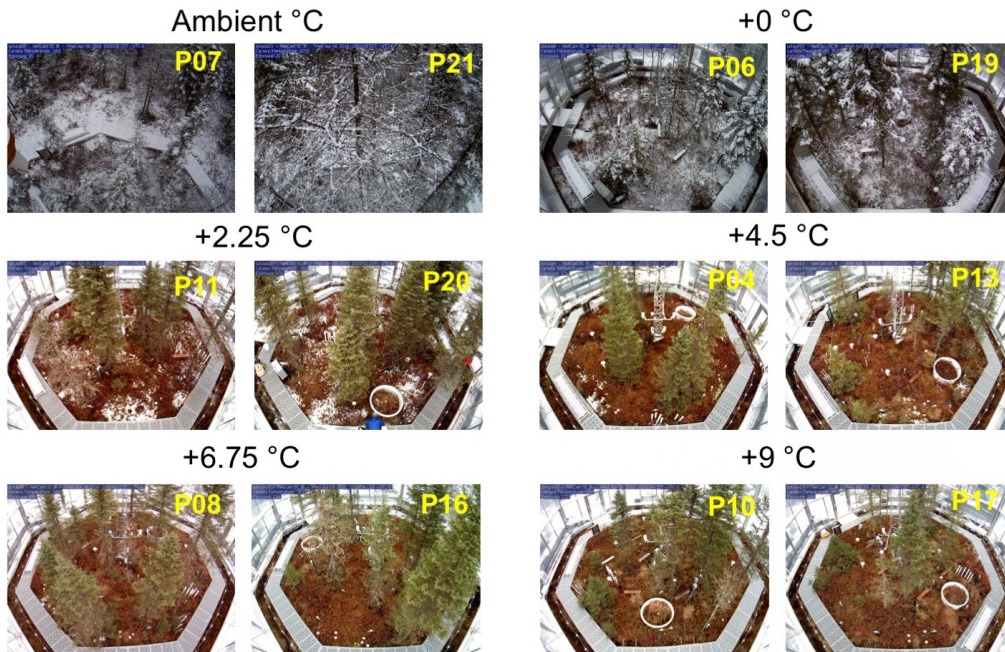
203  
204  
205  
206  
207  
208

**Figure S6:** Warm and cold season, seven-day example data for the diurnal variations in soil temperatures at -0.1 m. Calculated differentials with respect to reference Plot 6 are provided in the right hand column.



210  
211  
212  
213  
214  
215

**Figure S7:** Absolute humidity by treatment enclosure from mid-year 2015 through early 2016. For clarity of the image, standard error bars all in grey are included only for the control (T+0) and the warmest (T+9) plots.

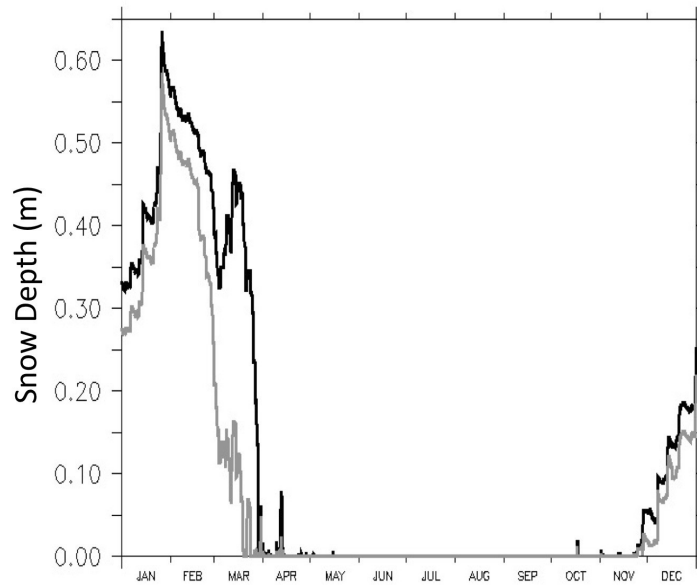


216  
217  
218  
219  
220  
221  
222

**Figure S8:** Images of snow accumulation at unchambered ambient locations and within all treatment enclosures by target warming temperature differentials at 10:00 on 6 April 2016. Little obvious snow accumulation is apparent above the +4.5 °C treatment, even though precipitation in the form of snow does enter all enclosures.

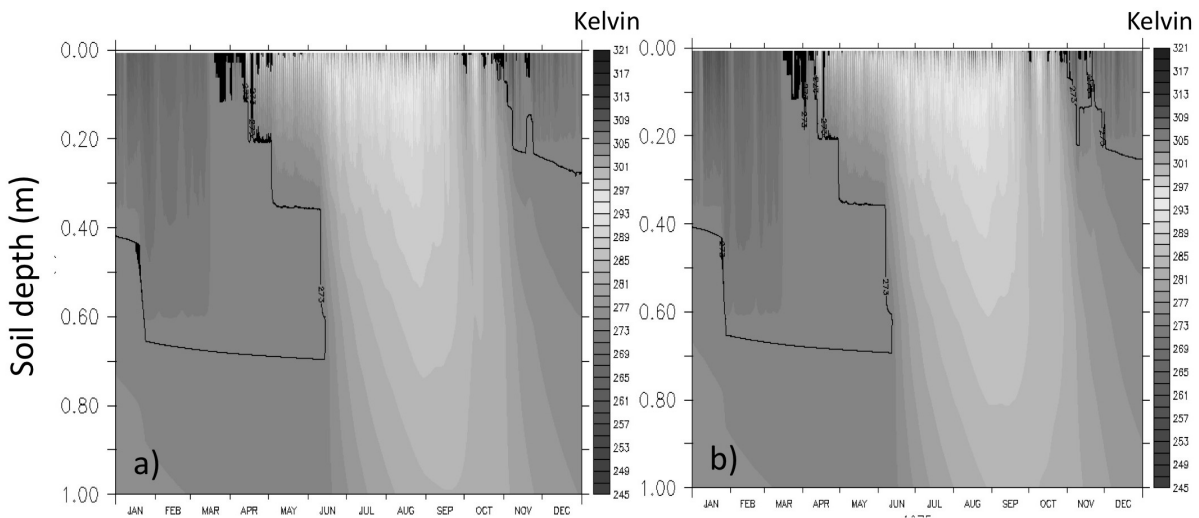
223  
224  
225

**Additional graphics from the SPRUCE Enclosure Energy Simulations (D. Ricciuto)**



226  
227  
228  
229  
230

**Figure S9:** Simulations of snow depth for ambient conditions (black) and within an enclosure (grey) using driver meteorology data from 2013.



231  
232  
233  
234  
235  
236

**Figure S10:** Profiles of simulated top 1m soil temperature in ambient (a) and enclosure (b) simulations. Contour colors represent peat temperatures in degrees kelvin, and the black contour indicates those layers that are below freezing during the year. Ice depths are similar between the simulations.

237 **Elevated CO<sub>2</sub> Protocol Details**

238  
 239 During the period from January through March 2016 when biological activities were minimal,  
 240 various test were conducted on Plot 19 (a constructed control), Plot 11 (+2.25 °C), Plot 4 (+4.5  
 241 °C), Plot 8 (+6.75 °C) and Plot 10 (+9 °C) to establish the CO<sub>2</sub> addition control protocols. Over a  
 242 multi-day period with variable winds, a fixed amount of CO<sub>2</sub> ranging from 150 to 300 l min<sup>-1</sup> of  
 243 pure CO<sub>2</sub>, depending on target temperature levels, was added to the enclosure for a multiple day  
 244 period to generate a profile of achieved CO<sub>2</sub> differentials (mean at 0.5, 1 and 2 m heights) as a  
 245 function of the wind velocities measured at +10 m. A fitted relationship between wind velocity at  
 246 +10 m and enclosure fractional air turnover volumes (assuming and enclosure volume of 911 m<sup>3</sup>)  
 247 was derived from these data. Instantaneous measured wind velocities were then applied to a  
 248 turnover fraction equation to estimate the amount of CO<sub>2</sub> to be added to achieve a +500 μmol  
 249 mol<sup>-1</sup> value over ambient-CO<sub>2</sub> measured within the constructed control plot (i.e., Plot 6). An  
 250 example is as follows:

251  $TF = (0.00001330297 * WS^6) + (-0.0003804215 * WS^5) + (0.003932579 * WS^4) +$   
 252  $(-0.01517648 * WS^3) + (-0.004974471 * WS^2) + (0.2532064 * WS)$

253 where TF is enclosure turnover fraction (unit less), and WS is wind velocity (m s<sup>-1</sup>). The form of  
 254 the TF equation might also be a simple exponential function depending on the calibration data  
 255 set for a given plot.

256  
 257 Using the TF value, an initial coarse control value for CO<sub>2</sub> addition was calculated as:  
 258 Course CO<sub>2</sub> Addition = CCO<sub>2</sub> = EV \* TF \* DeltaCO<sub>2</sub> \* 1000  
 259 where CCO<sub>2</sub> is the CO<sub>2</sub> addition rate in l min<sup>-1</sup>, EV is the enclosure volume in m<sup>3</sup> (~910 m<sup>3</sup>),  
 260 DeltaCO<sub>2</sub> is the desired target increase in CO<sub>2</sub> above ambient conditions (500 μmol mol<sup>-1</sup> or  
 261 0.0005 m<sup>3</sup> m<sup>-3</sup>), and 1000 allows for the conversion from m<sup>3</sup> to liters. To further account for the  
 262 variation in enclosure turnover times with external winds the DeltaCO<sub>2</sub> values were  
 263 supplemented with added amounts as shown in the following table.

264  
 265 Table S4. DeltaCO<sub>2</sub> adjustment values for low, medium and high winds by treatment plot.

CO <sub>2</sub> Treatment Plot #	Low Wind Adjustment (ppm)	Medium Wind Adjustment (ppm)	High Wind Adjustment (ppm)
4	50	50	50
10	125	75	40
11	75	75	75
16	50	25	0
19	75	50	0

266  
 267 Yet additional fine control to achieve target differential CO<sub>2</sub> concentrations within the enclosure  
 268 was based on a feedback adjustment defined by the error in achieving +500 μmol mol<sup>-1</sup>.  
 269 CO<sub>2</sub>ERR = 500 – (CO<sub>2</sub>Enclosure – CO<sub>2</sub>Ambient)

270  
 271 Final CO<sub>2</sub> Addition = FCO<sub>2</sub> = (910.6 \* CO<sub>2</sub>ERR)/1000000\*1000\*1.15  
 272 where CO<sub>2</sub>ERR is the observed difference of enclosure CO<sub>2</sub> when compared with CO<sub>2</sub> in the  
 273 constructed control (Plot 6), 1000000 and 1000 convert m<sup>3</sup> to L, and 1.15 is an arbitrary valued  
 274 needed to achieve good results (probably accounting for unmeasured vertical winds). This

275 combined control algorithm reevaluated every 10 seconds during active CO<sub>2</sub> additions, allowed  
 276 us to achieve target CO<sub>2</sub> levels within the enclosure within a  $\pm 50 \mu\text{mol mol}^{-1}$  band around our  
 277 target of + 500  $\mu\text{mol mol}^{-1}$  CO<sub>2</sub>. We will continue to adjust the algorithm for CO<sub>2</sub> additions as  
 278 we operate to allow each enclosure to achieve  $+500 \pm 25 \mu\text{mol mol}^{-1}$  for all wind conditions and  
 279 temperature treatments.

280  
 281 Elevated CO<sub>2</sub> additions are only made during daytime hours as a cost reducing measure, because  
 282 past studies have shown that there is no direct effect of elevated CO<sub>2</sub> on respiratory processes  
 283 (Amthor 2000; Amthor et al. 2001; Tjoelker et al. 2001). The elevated CO<sub>2</sub> treatments are  
 284 initiated or stopped each day based on calculated solar angles for each day of the year using the  
 285 Solpos algorithm developed by the National Renewable Energy Laboratory (NREL).

286  
 287 Table S5. Mean daily differential CO<sub>2</sub> achieved from 19 August to 1 September 2016. NA = not  
 288 applicable.

Warming Level and Plot	Differential [CO <sub>2</sub> ] in ppm $\pm$ sd
Reference Plot - +0.00 °C Plot 06	NA
+2.25 °C Plot 20	-9 $\pm$ 8
+4.50 °C Plot 13	-0.1 $\pm$ 8
+6.75 °C Plot 13	-13 $\pm$ 9
+9.00 °C Plot 04	1 $\pm$ 11
eCO <sub>2</sub> +0.00 °C Plot 19	483 $\pm$ 22
eCO <sub>2</sub> +2.25 °C Plot 11	471 $\pm$ 21
eCO <sub>2</sub> +4.50 °C Plot 04	490 $\pm$ 13
eCO <sub>2</sub> +2.25 °C Plot 16	511 $\pm$ 15
eCO <sub>2</sub> +9.00 °C Plot 10	480 $\pm$ 73

289

290

291 Supplemental Literature

292 Amthor, J.S.: Direct effect of elevated CO<sub>2</sub> on nocturnal in situ leaf respiration in nine temperate  
 293 deciduous tree species is small. *Tree Physiol.* 20, 139-144, 2000.

294

295 Amthor, J.S., Koch, G.W., Willms, J.R., Layzell, D.B.: Leaf O<sub>2</sub> uptake in the dark is independent  
 296 of coincident CO<sub>2</sub> partial pressure. *J Exper Bot*, 52, 2235–2238, 2001.

297

298 Tjoelker, M.G., Oleksyn, J., Lee, T.D., Reich, P.B.: Direct inhibition of leaf dark respiration by  
 299 elevated CO<sub>2</sub> is minor in 12 grassland species. *New Phytol*, 150, 419–424. doi:10.1046/j.1469-  
 300 8137.2001.00117.x, 2001.